

Climatic oscillations effect on the yellowfin tuna (*Thunnus albacares*) Spanish captures in the Indian Ocean

José Carlos Báez^{1,2}  | Ivone A. Czerwinski^{3,4}  | María Lourdes Ramos⁵

¹Centro Oceanográfico de Málaga, Instituto Español de Oceanografía, Fuengirola, Spain

²Facultad Ciencias de la Salud, Universidad Autónoma de Chile, Providencia, Chile

³Departamento de Biología, Facultad de Ciencias del Mar y Ambientales, Universidad de Cádiz, Cádiz, Spain

⁴Centro Oceanográfico de Cádiz, Instituto Español de Oceanografía, Cádiz, Spain

⁵Centro Oceanográfico de Canarias, Instituto Español de Oceanografía, Santa Cruz de Tenerife, Spain

Correspondence

José Carlos Báez, Instituto Español de Oceanografía, Centro Oceanográfico de Málaga, Puerto Pesquero de Fuengirola s/n, 29640 Fuengirola, Spain.
Email: granbaez_29@hotmail.com

Funding information

IEO project, Grant/Award Number: INDROP6; European Maritime and Fisheries Fund (EMFF), within the National Program of collection

Abstract

The yellowfin tuna (*Thunnus albacares*) (YFT) is among the eight marine species with the highest catches globally. The Spanish purse seine freezer fleet operating in the Indian Ocean is one of the most important YFT fishing fleets in the world. The South Oscillation Index (SOI), Pacific Decadal Oscillation (PDO), and Indian Ocean Dipole (IOD) are interrelated, and have combined effects in the Indian Ocean. Moreover, Madden–Julian Oscillation (MJO) is the dominant component of intraseasonal variability in the tropical Indian and Pacific oceans where the sea surface is warm. The main aim of present study is to understand the effect of these four climatic oscillations on Spanish purse seine YFT catches in the Indian Ocean. The ultimate goal is to estimate the specific time lag of the effect of each climatic oscillation on the YFT catches for management purposes. To estimate this, we adjusted different General Additive Models between the response variable (corrected YFT catches per unit of effort per year), compared to a combination of SOI, PDO, IOD, and MJO lagged up to 8 years. Our results suggest that there is a lagged effect modulated mainly by PDO–SOI, which could be related to a good recruitment, larval survival, or improved spawning. Thus, negative PDO phase (or positive SOI phase) lagged between 3 and 6 years could favor future stock abundance, while positive PDO phase (or negative SOI phase) lagged 3 or 6 years could negatively affect future stock abundance.

KEYWORDS

climatic oscillation, Indian Ocean, IOD, MJO, PDO, SOI, yellowfin tuna

1 | INTRODUCTION

Tuna species were one of the four most valuable fishing classes (together to lobsters, shrimps, and cephalopods) in 2014 (FAO, 2016), and they are considered an important contributor to global food security (Báez, Pascual-Alayón, Ramos, & Abascal, 2018). During 2014, the total catches of tuna and tuna-like species reached a new record, with almost 7.7 million tonnes caught and delivered to market (FAO, 2016). The yellowfin tuna (*Thunnus albacares*) (YFT) is among the eight marine species with the highest catches globally (FAO, 2016). The Spanish purse seine freezer fleet operating in the Indian Ocean is of the fleets with most YFT catches globally. It consists of a total

of 15 fishing boats supported by 6 non-fishing vessels, mainly managing the floating objects stock (deployment, detection, tuna school estimation, etc.). During 2014, the Spanish purse seiners from Indian Ocean caught 3.95% of the yellowfin tuna tonnes landed worldwide (data deducted from Báez et al., 2017).

The “Instituto Español de Oceanografía” (IEO) in Spain is responsible for producing scientific estimates of catch, effort, and other biological data for the Spanish purse seine fleet. Since 1990, the annual catch by species from Spanish purse seine freezer fleet operating in the Indian Ocean has been reported to the Indian Ocean Tuna Commission (IOTC) (see Báez et al., 2018 for the latest available report).

Currently, the YFT stock is subject to a wider plan for the reconstruction of the Indian Ocean tuna stock (described in the IOTC, 2016). In this context, understanding the natural variability of the stock and analyzing the response of the stock to climatic oscillations become necessary.

Many authors have suggested that climatic teleconnections (i.e., climatic oscillations with a seesaw effect, which generate an effect in one area, and show the opposite effect in distant areas) explain ecological processes better than single climate variables, since the climatic oscillations affect multiple weather variables simultaneously and their ecosystem responses (Bastos et al., 2016). Thus, climatic oscillations could explain fisheries fluctuations via both the capturability and changes in the local abundance (for example Chavez, Ryan, Lluch-Cota, & Ñiquen, 2003; Mantua & Hare, 2002; Rubio, Macías, Camiñas, Fernández, & Báez, 2016).

Atmosphere–ocean variability patterns are explained by teleconnections at both global and regional scales. At global scale, the El-Niño/Southern-Oscillation (ENSO) drives the climatic variability in the adjacent tropical Indian Ocean, although its effect could be bidirectional (Banu et al., 2015; Wieners, Dijkstra, & De Ruijter, 2017). The ENSO generates irregular fluctuations of the Sea Surface Temperature (SST), with a cold phase (La Niña) and a warm phase (El Niño), while the Southern Oscillation Index (SOI) shows the atmospheric oscillation coupled with ENSO. Thus, the SOI is considered a proxy of the ENSO, modulating the development and intensity of El Niño or La Niña events in the Pacific Ocean (Yan et al., 2011). The SOI is calculated using the pressure differences between the Tahiti and Darwin stations.

The Pacific Decadal Oscillation (PDO) is the result of a combination of different physical processes, including atmosphere–ocean interactions, which drive the SST North Pacific anomaly patterns (it is possible to see a revision in Newman et al., 2016). PDO-ENSO combinations could affect dry–wet patterns in remote areas in the Pacific Ocean (Wang, Huang, He, & Guan, 2014). Moreover, recent studies reveal that the subsurface cooling trend in the South Indian Ocean is mainly driven by remote PDO forcing, which could be related to other oceanographic phenomena in the Indian Ocean (Zhou, Alves, Marsland, Bi, & Hirst, 2017). At regional level, the Indian Ocean Dipole (IOD) is a coupled ocean–atmosphere phenomenon in the Indian Ocean. The IOD is considered a dipole, that is, a coupled ocean and atmosphere phenomenon instead of an atmospheric oscillation. The IOD is the leading driver of inter-annual variability of sea surface temperature (SST), typically during boreal summer and autumn, based on the empirical orthogonal function (EOF) analysis of SST anomalies. The IOD significantly affects the climate of the Indian Ocean-rim countries such as those along eastern Africa, India, and Indonesia (Lim & Hendon, 2017). Recent studies reveal that both ENSO and IOD drive the tuna fisheries yield from Indian Ocean (Kumar, Pillai, & Manjusha, 2014; Marsac & Demarcq, 2016).

The Madden-Julian Oscillation (MJO) is not a teleconnection (i.e., the MJO does not show the seesaw response), but is the dominant driver of the intraseasonal variability in the tropical Indian and Pacific oceans where the sea surface is warm (Zhang, 2005).

Unlike a typical teleconnection (such as the SOI or PDO), the MJO is a traveling pattern related to the coupling eastward propagation of general atmospheric circulation, generating convection wind in tropical areas and atmospheric variability. Both Kelvin and Rossby wave structures have been considered dynamically essential to the MJO (Zhang, 2005). This overall circulation pattern manifests itself most clearly as anomalous rainfall. The MJO is estimated using an EOF that combines cloud amount and winds at upper and lower levels of the atmosphere, and this function depends on the longitude (Wheeler & Hendon, 2004). For this reason, as longitude 80°E represents the limit of Western and Eastern Indian Ocean according to the IOTC, the MJO 80°E (hereafter MJO80E) was considered in this study.

From a stock management point of view, it could be important to know in advance the macroecological processes that could be coupled to the dynamics of YFT populations, and consequentially adopt pre-emptive fisheries management rules, to minimize these effects. In this sense, the main aim of the present study is to investigate the possible lagged effect of the four atmospheric climatic oscillations (PDO, SOI, IOD, and MJO) on Spanish purse seine YFT catch in the Indian Ocean.

2 | MATERIAL AND METHODS

2.1 | Fishery data

The Spanish purse seine fishery in the Indian Ocean is an industrial fishery that targets a mixture of tuna species, mainly skipjack tuna (*Katsuwonus pelamis*) (SKJ), yellowfin tuna (*Thunnus albacares*) (YFT), and bigeye tuna (*Thunnus obesus*) (BET). In this context, it is very difficult to determine the real catch composition by species. This is a problem that has been known for many years (i.e., Fonteneau, 1976; Pallares et al., 1983; Pianet et al., 2000). Consequently, a correction procedure, based on a multi-species sampling system in port, was designed for the landings registered in the logbook by species. This methodology has been used since 1984 in the major unloading ports of the EU of the Indian Ocean (Pianet et al., 2000) and is conducted annually by the Spanish fleet. Sampling operations are conducted during the unloading of the purse seiners at fishing ports to estimate the size and species composition of the catch. The species composition rates found are applied to geographic strata (5°x5° areas), and these values are weighted by the total catch. We used the annual corrected YFT catch in this study (for a more details and data description see Báez, Pascual-Alayón, et al., 2018).

Industrial purse seine vessels use high-tech devices to target tunas, such as FADS, which can be attached with satellite buoys equipped with echosounders to provide information to skippers about the fish schools under the FADs. Moreover, the purse seiners are also supported by non-fishing vessels that mainly deploy FADs, and perform detection of tuna schools. These technologies have changed over time making it difficult to weight the fishing effort of the fleet by year. However, the time spent in fishing-related

activities (i.e., searching, installing FADs, or fishing operations such as setting, hauling, and removing catches from the fishing gear) by the fleet per boat and year, expressed as the number fishing days, is a good proxy to the fishing effort. Thus, we defined the yellowfin tuna (YFT) Catches per Unit Effort (CPUE) as the Spanish freezer fleet's corrected annual catch per fishing days (f.day) from 1990 to 2018.

2.2 | Climatic indices

The atmospheric climatic oscillation indices evaluated were as follows: PDO, SOI, IOD, and MJO. Climatic indices values were provided by the NOAA (National Oceanic and Atmospheric Administration) website, with the exception of the PDO. We used the classic estimation proposed by Mantua, Hare, Zhang, Wallace, and Francis (1997) for the PDO index, available at <http://research.jisao.washington.edu/pdo/PDO.latest.txt> (last accessed on 14/02/2020). The SOI values are available at <https://www.ncdc.noaa.gov/teleconnections/enso/indicators/soi/> (last accessed 14/02/2020).

Multiple climatic indices could have a combined effect on the ocean (Báez, Gimeno, Gómez-Gesteira, Ferri-Yáñez, & Real, 2013). In this sense, Wang et al. (2014) found a combined effect of PDO and SOI on the air pressure and dry-wet variations of the overlying atmosphere on Indian Ocean. For this reason, we used the combination of the different climatic indices and lags in our explanatory models.

In the case of IOD, we used the fluctuation in the SST anomalies between the western equatorial Indian Ocean (50E-70E and 10S-10N) and the southeastern equatorial Indian Ocean (90E-110E and 10S-0N), which is called Dipole Mode Index, available at the website: https://www.esrl.noaa.gov/psd/gcos_wgsp/Timeseries/DMI/ (last access 14/02/2020).

The MJO80E is available at the website: https://www.cpc.ncep.noaa.gov/products/precip/CWlink/daily_mjo_index/proj_norm_order.ascii (last accessed on 14/02/2020).

Taking into account that the environmental variables may have a delayed effect on the CPUE, the aforementioned climatic indices (i.e., the SOI, IOD, PDO, and MJO80E) were lagged up to 8 years, as their values from the previous years are known, generating 9 variables of each of the four climatic oscillations, giving a total of 36 explanatory variables. We used a maximum lag of 8 years because the oldest YFT individual recorded in the Indian Ocean was ~9 years old (Rohit, Syda, & Rammohan, 2012). On the other hand, the climate index could have a cumulative effect on different cohorts. Báez, Ortiz De Urbina, Real, and Macías (2011) showed that NAO had a delayed and accumulated effect throughout the life of *T. alalunga*, which manifested in changes to local abundance.

2.3 | Data exploration

To begin with, YFT CPUE and the aforementioned climatic indices time series were analyzed for identifying multiple changepoints within the mean and variance of the time series using the *changepoint*

R package (Killick, Haynes, & Eckley, 2016). The binary segmentation (Edwards & Cavalli-Sforza, 1965) was the change point detection method chosen when applying the "cpt.meanvar" function, as it is the most widely used multiple changepoint search method (Killick & Eckley, 2014). A specific explanation of the method can be found in Killick, Fearnhead, and Eckley (2012). The non-parametric Mann-Kendall test (Kendall, 1955; Mann, 1945) was also applied to the environmental data to detect time series trends.

Moreover, in a first step to identify the explanatory variables with effect on the response variable YFT CPUE, we estimated Pearson's correlation coefficient with the climatic indices lagged up to 8 years. This analysis is similar to cross-correlations but without the handicap of losing data in each delay, since we know the values before 1990 for all climatic indices. The explanatory variables with an absolute correlation value with YFT greater than 0.1 were selected as variables with potential non-linear effects on YFT, and explored in a similar way to the one described in the protocol of Zuur, Ieno, and Elphick (2010). Secondly, a Pearson's correlation analysis was used to test for collinearity between explanatory variables in all possible pair combinations, to choose which explanatory variables were to be included together in models with two independent variables (Zuur et al., 2010), using a correlation value of 0.6 as a threshold (Lezama-Ochoa et al., 2017; Wood, 2006).

2.4 | GAM models

Generalized additive models (GAM) are non-parametric generalization of multiple linear regressions which are less restrictive in assumptions of the underlying statistical data distribution (Hastie and Tibshirani., 1990). In these models, the linear predictors are related to the response variables via a link function that extends the use of the regression models beyond non-Gaussian response variables. GAM uses data-driven functions, such as splines and local regression which have superior performance relative to the polynomial functions used in linear models (Diankha and Thiaw, 2016). They allow depicting complex non-linear relations between species and their environment (Zwolinski, Emmett, & Demer, 2011).

The GAM semi-parametric smooth functions (s) were used to fit the interactions between the climatic indices and YFT. There were adjusted twenty models with a single explanatory variable, and 183 models with two explanatory variables. In order to avoid collinearity, only pairs of variables with correlation less than 0.6 in absolute value were included together in the models. The Akaike information criterion (AIC) and a graphical validation of model residuals were used to select the best models (Zuur, Ieno, Walker, Saveliev, & Smith, 2009). Concurvity was also tested for models with two covariables, and an autocorrelation analysis of the residuals was performed.

The data exploration and statistical analyses were carried out with R (version 3.5.0), and GAM models were fitted using the *mgcv* library (version 1.8; Wood, 2011) in R.

3 | RESULTS

3.1 | Data exploration

The estimated yellowfin tuna CPUE time series reached the maximum value in 2003 of 18 t/ f.day, the minimum in 2007 of 6 t/ f.day with a mean of 12 t/ f.day for the entire time series (Figure 1). To describe the time series evolution, four main periods of YFT CPUE were identified in the changepoint analysis: the first and longest period, between 1990 and 2002 with a mean of 9.97 t/ f.day and the lowest variance (1.92), the second between 2003 and 2005 with the highest mean of 16 t/ f.day and the highest variance (3.67) as well, the third period between 2006 and 2009 with a mean of 9.5 t/ f.day and a high variance (3.51) and finally the period between 2010 and 2018 with a mean of 14.3 t/ f.day a lower variance (2.15).

South Oscillation Index annual mean (Figure 2) index varies between -0.9 (1987) and 1.4 (2011) with a total mean of 0.1. The time series shows two main periods estimated with the changepoint analysis with different means but similar variance. The first one, from 1980 to 1998, shows a negative mean value of -0.19 with a variance value of 0.315. During this 19 year period, negative extreme values of the time series are recorded in 1982 and 1987 and 13 years (68%) were in negative phase. The second period, from 1999 to 2018 (20 years), shows a positive mean value of 0.25 and a variance of 0.284, with only 7 years (35%) in a negative phase, with extreme positive values of the time series recorded in 2008 and 2011. The difference between the SOI periods suggests a slight positive trend in the time series, but the Mann-Kendall trend test does not confirm its significance ($p = .08$).

The PDO annual mean index (Figure 3) varies between -1.3 (in 2008) and 1.8 (in 1987) with a total mean of 0.2. The PDO time series shows five periods in the changepoint analysis. The first period coincides with the first SOI period from 1980 to 1998 but with a positive mean value of 0.65 and a variance value of 0.4. Only 4 of the 19 years (21%) were in negative phase. The second period, starting in 1999 and ending in 2001, shows all years in negative phase, with a mean value of -0.74 and a variance of 0.05. The third period, from

2002 to 2007, has only one year in negative phase (17%), and has a mean value of 0.32 and a variance value of 0.12. The fourth and the longest negative period, from 2008 to 2013, with all years in negative phase, shows the minimum value of the time series, with a mean value of -0.84 and a variance value of 0.14. Finally, the last and most positive period from 2014 to 2018 has a mean value of 0.75 with a high variance value of 0.75. Although the time series ends in a positive period, there is an overall negative trend, corroborated by the Mann-Kendall trend test with a p -value of .029.

Looking at the temporal coincidence of the first period of the SOI and PDO indices, the correlation between these two indices in the two SOI periods was analyzed separately. It should be noted that from 1980 to 1998, there was no significant correlation between SPI and PDO ($r = -0.28, p = .24$); however, from 1999 to 2018, the correlation between these two indices was strongly negative and highly significant ($r = -0.80, p < .001$).

Indian Ocean Dipole annual mean index (Figure 4) varies between -0.3 (1992) and 0.7 (1997) with a mean of 0.2. Only 5 years (15%) of the time series are in negative phase. The changepoint analysis reveals three main periods, each one with a mean value higher than the previous one, revealing a positive long-term trend with a

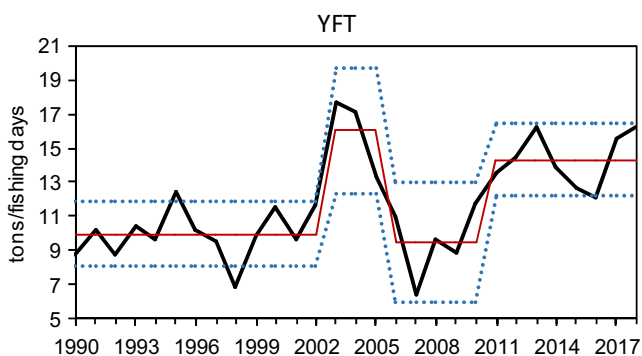


FIGURE 1 Yellowfin tuna annual CPUE from Spanish purse seine freezer fleet operating in the Indian Ocean. The red line defines the mean and the blue dotted line shows the variance in periods identified by the changepoint analysis

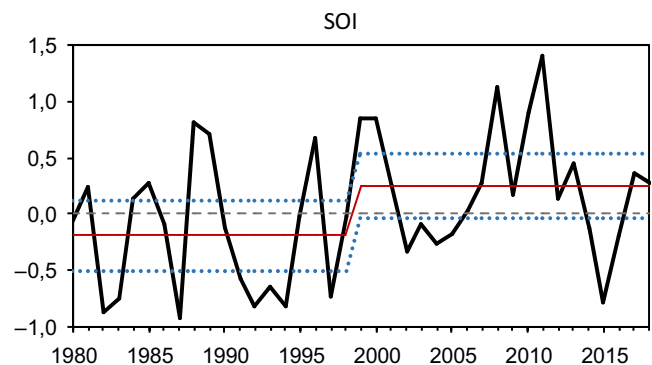


FIGURE 2 South Oscillation Index (SOI) annual mean indices time series. The red line defines the mean and the blue dotted line shows the variance in periods identified by the changepoint analysis

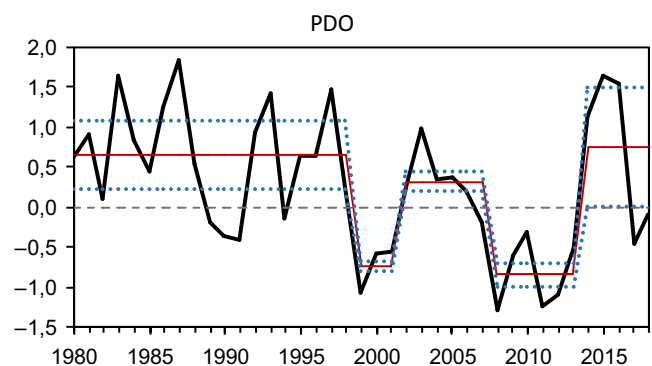


FIGURE 3 Pacific Decadal Oscillation (PDO) annual mean indices time series. The red line defines the mean and the blue dotted line shows the variance in periods identified by the changepoint analysis

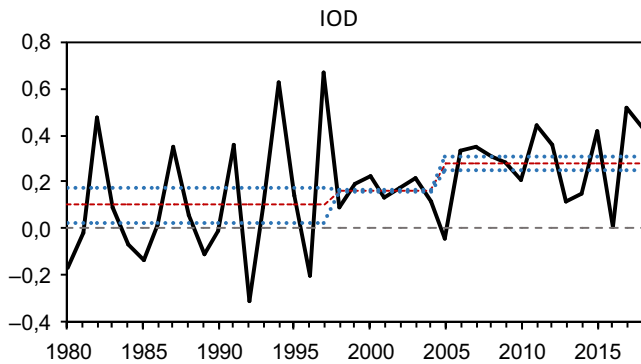


FIGURE 4 Indian Ocean Dipole (IOD) annual mean indices time series. The red line defines the mean and the blue dotted line shows the variance in periods identified by the chaingepoint analysis

variance decrease considerably in the last two periods. The first one, from 1980 to 1997, has a mean value of 0.10, the second one, from 1998 to 2004, has a mean value of 0.16, and the last one, from 2005 to 2018, has a mean value of 0.28.

MJO80E annual mean index (Figure 5) varies between -0.6 (1988) and 0.8 (2015) with a mean of -0.1 . The index shows frequent fluctuations between the negative and the positive phases, although negative phase years amount to 60% of the time series with periods lasting up to 4 years and positive ones up to 3 years. The change point analysis shows no changes in mean and variance along the time series, and the Mann–Kendall trend test shows no significant trend in this time series.

The changepoint analysis reveals a stable period in SOI, PDO, and IOD from 1980 to 1997–1998, when there is a shift in the three time series means. After this shift, the PDO index shows more variability than SOI and IOD, shifting from negative to positive means three more times.

The analysis of correlations of the YFT time series with the time series of the non-lagged and lagged climatic indices (lagged up to 8 years) (Table 1) shows significant correlations with SOI lagged 4 and 5 years, and insignificant although higher than 0.1 in absolute value correlations lagged 3, 6, and 7 years. The correlations of the

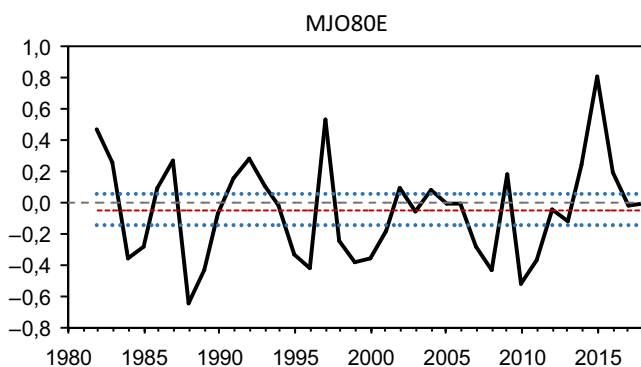


FIGURE 5 MJO80E annual mean indices time series. The red line defines the mean and the blue dotted line shows the variance in periods identified by the chaingepoint analysis

YFT with the PDO are negative, being significant in lags 4 and 5, and greater than 0.1 in lags 3, 6, and 8. The IOD climate index, however, shows only one significant correlation with the 6-year lag and correlations greater than 0.1 in almost all other lags except 1 and 4 years. MJO80E does not show any significant linear correlation, although it does exceed 0.1 in lags 2, 4, 5, and 7.

The time series of climatic indices show significant and greater than 0.6 absolute value linear correlations between the SOI and the PDO (-0.69), between SOI and MJO80E (0.80), and between the PDO and MJO80E (0.63), which is interpreted as collinearity among these pairs of variables (Figure 6). Seven of the 190 different pairs of explanatory variables tested (including all climatic indices lagged up to 8 years) were found to be collinear (Table 2), all of them with combinations of the PDO or MJO80E and SOI indices with the same time lag as was expected from the plain indices correlation analysis (Figure 6). These seven collinear pairs of variables were not included in the GAM models to avoid collinearity.

3.2 | GAM models

The best-performing GAM models were obtained using the Gaussian error structure and the identity link function.

The single independent variable model with best fit and AIC values was constructed with the PDO lagged 5 years (PDO5) with an adjusted R -squared value of 0.35 (Table 3, Mod.008). According to this model, the effect of the PDO lagged five years on yellowfin tuna CPUE is negative and almost linear as suggested the Pearson's correlation index value (-0.61) (Figure 7).

Models with two independent variables with the best AIC values included the PDO index lagged four or six years (Table 3). The model with the lowest AIC value (Mod.131) was fitted with the PDO lagged 6 years (PDO6) and the SOI lagged 3 years (SOI3) with an adjusted R -squared value of 0.689, explaining 83% of the deviance. According to this model, the single partial effect of PDO6 on YFT is negative when PDO6 has values from -1 to -0.5 (with the maximum value of YFT for $\text{PDO6} = -1$), for PDO6 values between -0.5 and 0, the partial effect becomes positive and returns to be negative for PDO values between 0 and 1 (with the lowest value of YFT for $\text{PDO6} = 1$). From the PDO6 value of 1 onwards, the partial effect on YFT is positive. In this same model, the partial single effect of SOI3 is less clear, with the lowest effect on YFT reached at the highest value of SOI3 (1.4), and two other minima produced at values close to 0.7 and -0.25 . The highest effect of YFT is reached at values close to 1, with a second maximum at values between 0 and 0.5 (Figure 8).

The second lowest AIC value (Mod.113) was obtained by combining the PDO lagged 6 years and the IOD lagged 3 years, with an adjusted R -squared value of 0.64% and 78% of deviance explained. In this model, the partial effect of PDO6 is similar to that obtained in the previous model (Mod. 131), although much more pronounced, with maximum effects at values close to -1 , 0, and 1.5 and minimum effects at values close to -0.5 and 1. On the other hand, the partial effect of the 3-year lagged IOD index (IOD3) on YFT shows a

TABLE 1 Pearson's correlation coefficients for each lag of the climatic indices with the yellowfin tuna CPUE time series

Lag	SOI	PDO	IOD	MJO80E
0	0.095	0.058	0.107	0.099
-1	0.052	-0.070	0.074	0.056
-2	0.040	-0.068	0.250	0.221
-3	0.287	-0.251	0.158	0.068
-4	0.518**	-0.548**	0.078	-0.220
-5	0.457*	-0.612***	0.241	-0.314
-6	0.227	-0.311	0.509**	-0.029
-7	0.284	-0.007	0.167	-0.139
-8	0.039	0.155	0.056	-0.028

Note: Correlation coefficients with absolute values greater than 0.1 in bold.

Signif. Codes: 0.001 "****" 0.01 "***" 0.05 "**".

TABLE 2 Pearson's correlation coefficients for pairs of explanatory variables found to be collinear

Pairs of explanatory variables		Pearson's correlation coefficient
PDO3	SOI3	-0.686
PDO4	SOI4	-0.650
MJO80E4	SOI4	-0.838
PDO5	SOI5	-0.646
MJO80E5	SOI5	-0.847
PDO6	SOI6	-0.631
MJO80E7	SOI7	-0.854

Note: These pairs of explanatory variables were not included in GAM models.

Signif. Codes: 0.001 "****" 0.01 "***" 0.05 "**" (see results for all tested pairs in complementary material).

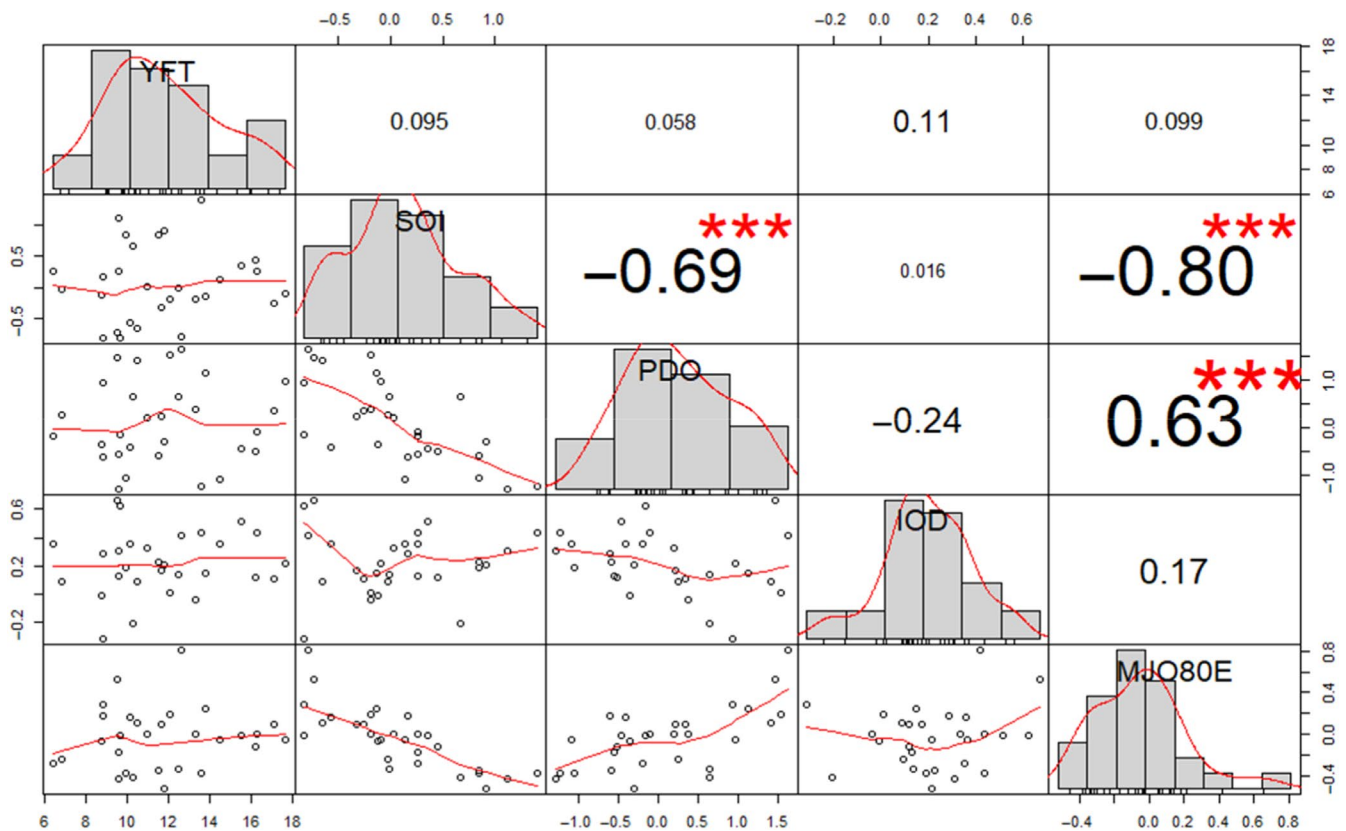


FIGURE 6 Correlation Matrix Chart of yellowfin tuna CPUE and climatic indices. Bivariate scatterplots, with a fitted line (lower panel), single variable histograms and Kernel density (diagonal), Pearson correlation coefficient and Signif.Codes: 0 "****" 0.001 "***" 0.01 "**" 0.05 "*" 0.1 " " 1 (upper panel)

maximum at values close to 0.3 and minimum at values close to -0.1 and above 0.6 (Figure 9).

The third lowest value of AIC (Mod.085) was found in an additive combination of the PDO and the MJO80E lagged both four years (MJO80E4 and PDO4), with an adjusted R-squared value of 0.635% and the 78.8% of the deviance explained. Partial single effects of these climatic indices on yellowfin tuna CPUE are different. The four years lagged PDO partial effect on YFT is negative

and almost linear from a value close to -0.5 to 1. However, the four years lagged MJO80E partial effect reaches its minimum in values close to 0 and shows two maxima in values close to -0.4 and 0.4 (Figure 10).

Residuals of the three best bivariate models were found to be normally distributed and with no autocorrelation (see Shapiro-Wilk test results and residuals autocorrelation plots in additional material).

TABLE 3 Significant covariates, degrees of freedom goodness of fit (Akaike Information Criterion AIC), model performance with deviance explained in percentage and regression coefficient R-sq. adjusted are shown for GAM selected models

Model	Covariates	Degrees of freedom	AIC	Deviance explained	R ² adjusted
Mod.008	PDO5	3,000	136.5	0.374	0.351
Mod.131	PDO6, SOI3	15,101	122.1	0.834	0.689
Mod.113	IOD3, PDO6	12,779	125.7	0.780	0.643
Mod.085	MJO80E4, PDO4	13,679	126.6	0.787	0.635

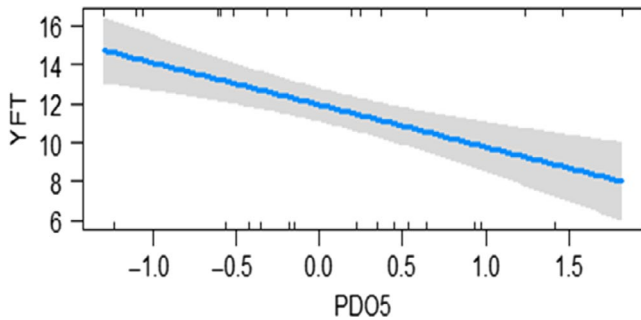


FIGURE 7 Generalized additive model (GAM) derived effect of the climatic index PDO lagged 5 years on yellowfin tuna CPUE (Model 008). Shaded area indicates 95% of the confidence intervals. The relative density of data points is shown in rugs plot along the x-axis

The combined additive effect of climatic indices on yellowfin tuna CPUE shows similar patterns for each of the selected models (Figure 11). The model with SOI3 and PDO6 (Mod.131) predicted the highest values for yellowfin tuna CPUE for SOI3 = 1 (positive phase) and PDO6 < -1 (negative phase). However, the model constructed with PDO6 and IOD3 (Mod.113) expects highest CPUE values for

IOD3 values between 0.2 and 0.4 combined with either extreme values of PDO6 or PDO6 = 0. On the other hand, the model with both climatic indices lagged four years (Mod.085) shows the highest expected CPUE values for PDO4 between -1 and -0.5 and MJO80E4 close to either -0.4 or 0.4.

4 | DISCUSSION

The time series of SOI, PDO, and IOD show stability in their mean and variances until a shift in the years 1998–1999. From there, PDO and IOD show periods of different phases with greater frequency. It is worthy of note that the YFT time series has a similar behavior, although with a few years of lag, showing some stability until 2002 and more frequent period changes since then.

GAM results suggest that climatic indices and combinations of them could be key in yellowfin tuna CPUE long-term forecasting. Considering the independent effects of each of the analyzed indexes, linear effects can be seen in the results of the correlation analysis with YFT (Table 1), in which it is observed that both PDO and SOI have their maximum correlations with YFT with 4 and 5 years of lag,

FIGURE 8 Generalized additive model (GAM) derived partial single effect of the 6 years lagged PDO and 3 years lagged SOI climatic indices on yellowfin tuna CPUE (Model 131). Shaded area indicates 95% of the confidence intervals. The relative density of data points is shown in rugs plot along the x-axis

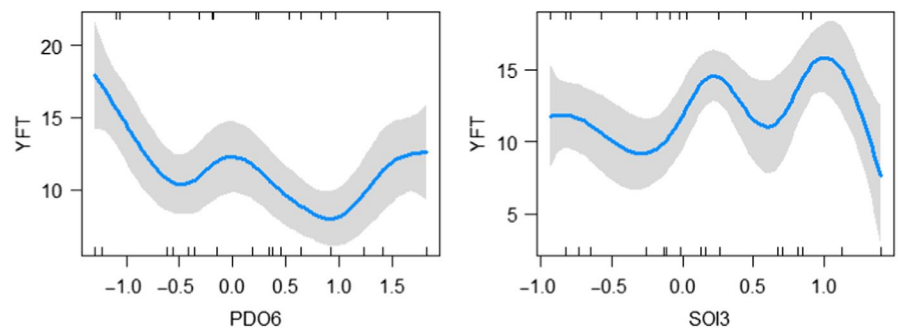
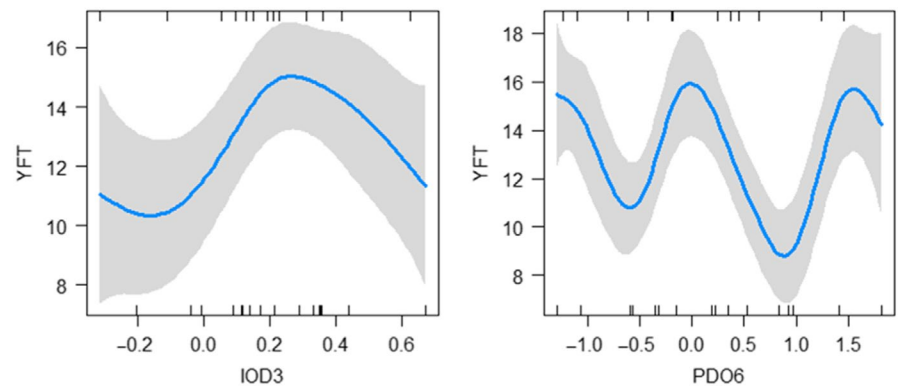


FIGURE 9 Generalized additive model (GAM) derived partial single effect of the 3 years lagged IOD and the 6 years lagged PDO climatic indices on yellowfin tuna CPUE (Model 113). Shaded area indicates 95% of the confidence intervals. The relative density of data points is shown in rugs plot along the x-axis



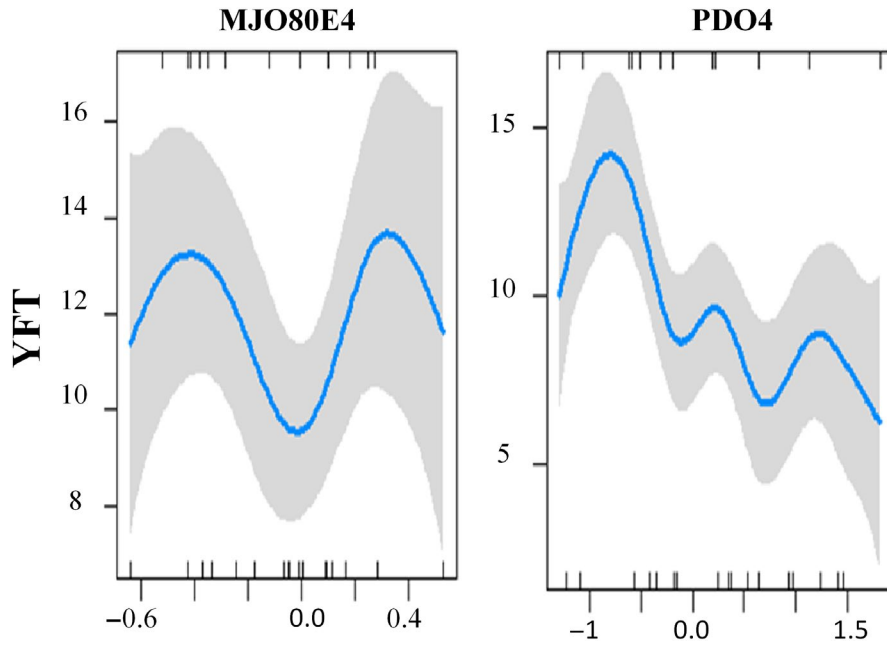


FIGURE 10 Generalized additive model (GAM) derived partial single effect of the climatic indices PDO and MJO80E lagged four years on yellowfin tuna CPUE (Model 085). Shaded area indicates 95% of the confidence intervals. The relative density of data points is shown in rugs plot along the x-axis

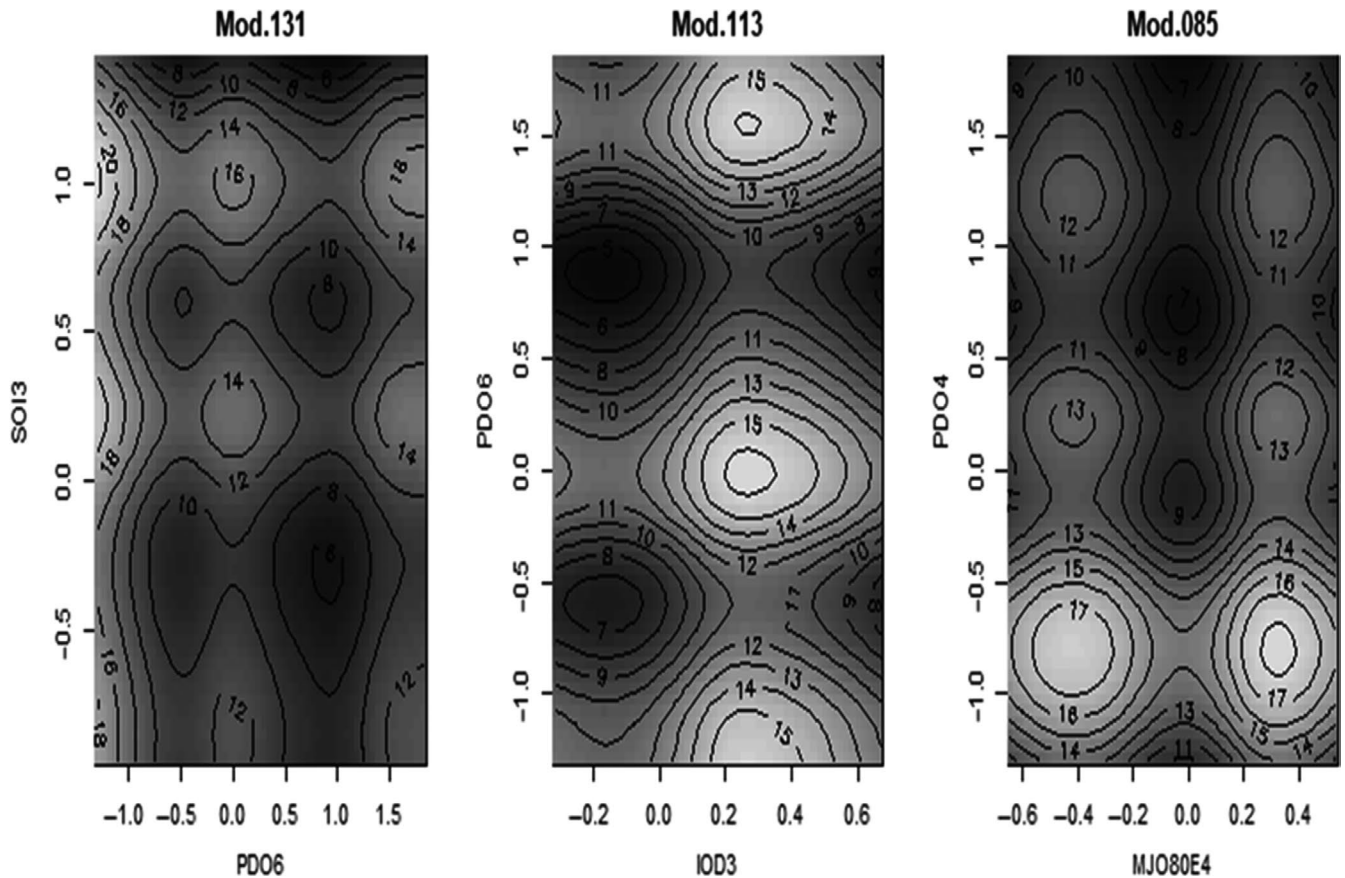


FIGURE 11 Generalized additive model (GAM) derived additive effect of the climatic indices on yellowfin tuna CPUE (t/f.day) following the three selected models (contour lines indicate the estimated CPUE values; the lighter shades of gray correspond to higher CPUE values)

and IOD with a lag of 6 years. GAMs with a single explanatory variable obtained better results with PDO delayed 4 and 5 years (see additional material), confirming the linear effect of this variable. These results also indicate that 4 or 5 years after a negative phase of PDO

we would expect high YFT values, whereas after a positive phase of PDO, it would be expected otherwise. In GAMs with only SOI, the best result is obtained with SOI4, and in models with only IOD, the best result is obtained with IOD6, both indices with the same lag

in which linear correlations with YFT are significant. This changes when the possible combined effects between different indices are taken into account using GAMs with two explanatory variables. The best models are obtained with lags of the indices that do not have a significant linear correlation with YFT, suggesting that the combined effects are non-linear.

The PDO index turned out to be a significant variable in the models with better AIC values indicating that it is the most relevant index to forecast YFT. Taking into account the correlation between PDO and SOI, it would be expected that both variables were equally significant in the models; however, the correlation between PDO and SOI has changed over time, and this is likely to affect the fit with YFT. Even so, the model with the lowest AIC (Mod.131) includes both indices with different lags (SOI3 and PDO6), which may indicate that the climatic effect that each of them represents has its effect at different times in the life and fishing history of this species. According to the results of the two models with the best AIC value (Mod.131 and Mod.113), PDO would have a partial effect with a delay of 6 years and there would be a partial effect of other indices such as SOI or IOD with a delay of 3 years. In both models, the YFT maximums are given with the same PDO6 values (PDO6 <-1, PDO6 = 0 and PDO > 1.5). The two models agree that the second index with partial effect on YFT would have 3 years lagged effect. In the third model with the best AIC value (mod.85), we found an intermediate delay in the expected effects located in four years for PDO and MJO80E. Taking into account the results of these three models and models with a single explanatory variable, we could deduce that a close estimate of YFT could be obtained from PDO values delayed between 4 and 6 years, combined with a second index delayed between 3 and 4 years. This gives us a time range between 3 and 6 years in which climatic variations would have an effect in the future on yellowfin tuna catches.

According to Ménard, Marsac, Bellier, and Cazelles (2007), the IOD could be the most important climatic oscillation affecting tuna catch. We observed that the PDO could be more important than the IOD to explain YFT catch variability in the Indian Ocean. Lagged PDO could explain an important portion of the observed variability of the data.

Faillietaz, Beaugrand, Goberville, and Kirby (2019) found long-time lagged effect to up 16 years with Atlantic Multidecadal Oscillation (AMO) and North Atlantic Oscillation (NAO) for the Atlantic bluefin tuna (*T. thynnus*). Here, we have not used such large lags, because we have restricted ourselves to a single generation. In addition, fishing mortality is much higher in the case of the YFT for the Indian Ocean, than for bluefin tuna (417,000 t on average between 2014 and 2018), so the high fishing mortality would prevent detection of the effects on multiple generations.

The effect of climatic oscillation is related to the phase (positive or negative sign) of the indices. In this sense, PDO and SOI (at the same time strongly related to ENSO) are strongly negatively correlated. Thus, we expect that the negative PDO phase or positive SOI phase has a similar effect on YFT catch as the positive PDO phase

or negative SOI phase. Moreover, an extreme signal from climatic oscillation could intensify the effect (Vicente-Serrano et al., 2011). In relation to this, we observed that the 2 years with the highest CPUE of the series (years 2003; 2004) correspond to highly negative values of the PDO4 and positive extreme phases of SOI4. The mean CPUE during negative PDO4 phases was 13.3 t/f.day versus 10.3 t/f.day during positive phases.

In a general context, the ENSO/SOI could affect directly the catchability of YFT (therefore PDO too), by modifying the sea surface temperature and therefore the thermocline. In a recent article, Yang et al. (2019) showed that the ENSO events impact on the thermocline variability in the Southern Tropical Indian Ocean. In this sense, according to a report of the IATTC (2015), the effect of the ENSO on the catchability of BET is acknowledged from eastern Pacific Ocean, as it can alter the depth of the thermocline. Likewise, Rubio et al. (2016) highlighted the effects of the NAO, another important atmospheric oscillation in the catchability of YFT from the Atlantic Ocean. However, this cannot explain the multi-year lag in its effect.

Many studies have analyzed the effect of climatic oscillations on tropical tunas, and they have identified effects on their abundance (Kumar et al., 2014; Lima & Naya, 2011), reproductive condition (Kanaji, Tanabe, Watanabe, Oshima, & Okazaki, 2012; Kim, 2015), recruitment to the fisheries (Lehodey, Chai, & Hampton, 2003; Mejuto, 2003; IATTC 2016), and distribution (Faillietaz et al., 2019). Báez et al. (2011) conclude that the atmospheric oscillations North Atlantic Oscillation (NAO) could affect the physical condition of albacore (*T. alalunga*) from the Mediterranean Sea. Moreover, NAO has a cumulative effect throughout its biological cycle, affecting the number of spawn sessions that albacores can perform throughout their lives, which could be extended to other tuna species. Taking this evidence into account, a possible explanation for observed delay between PDO-SOI and YFT catch could be related to with a cumulative effect on YFT physical condition and spawns intensity. However, there are no studies on YFT physical condition and spawns intensity in relation to climatic oscillations from Indian Ocean.

In relation to recruitment of the YFT to the fishery, there are no direct measurements of YFT recruitment to the population. Langley, Briand, Kirby, and Murtugudde (2009) used estimates of recruitment strength, available in assessment models, to determine the relevance of the oceanic variability in tuna's recruitment at different spatio-temporal ENSO scales of the Western-Central Pacific Ocean. Langley et al. (2009) and Torres-Faurrieta, Dreyfus, and Rivas (2016) concluding that the YFT recruitment in the Pacific Ocean is driven by the variability in the spatial extent of the warm pool, which tends to occur during El Niño conditions (i.e., negative SOI). These findings appear to be in opposition to our results, but recent oceanography studies show that during the El Niño (i.e., negative SOI), cold SST anomalies appear and intensify in the east of tropical Indian Ocean (Hu, Wu, & Wu, 2018). Thereby, our results are in consistency with previous findings from Pacific Ocean, confirming that the PDO-SOI must have an effect

on the recruitment. According to Faillettaz et al. (2019), the AMO and NAO drive the distribution of bluefin tuna from North Atlantic Ocean affecting its distribution and local abundance. Thus, a similar way lagged PDO could affect the distribution and local abundance of YFT from Indian Ocean. This explanation seems less plausible, since the purse seine fleet performed an intense search together with its supply vessels, so a change in the distribution of the YFT schools would be followed by a displacement of the fleet in its search, and this has not happened. Finally, we concluded that a multi-year lag effect on the recruitment and/or a cumulative effect on YFT physical condition and spawns intensity could be the explanation of our findings. However, we do not know which of the two hypotheses is the correct explanation, or if there is a combination of both.

Robison et al. (2009) suggested that climate variability could affect the local Seychelles economy, due to its dependence on tuna fishing activity. Our study demonstrating a lag between the effect of climatic oscillations and its effect on the fishery could be used to help inform management in such contexts. There are some studies in the area on the effect of climate oscillations on tropical tuna catches (Robison et al., 2009; Ménard et al., 2007; Marsac & Demarcq, 2016; Erauskin-Extramiana et al., 2019); however, the effect of PDO has been poorly tested. For example, Erauskin-Extramiana et al. (2019) do not consider that the PDO affect the YFT stock from Indian Ocean. However, these authors found negative correlation between PDO and changes in the distribution of YFT stock from Eastern Pacific Ocean.

The present study demonstrates the importance of the effect of the PDO and highlights the teleconnection between the Pacific and the Indian Ocean.

Currently, the planet is experiencing rapid global warming, and one effect is to more frequently achieve extreme values for climatic indices (Vicente-Serrano et al., 2011). In this paper, we show that the extreme values of the indices could increase/decrease catches of tropical tunas.

ACKNOWLEDGEMENTS

This study was supported by IEO project INDROP6 and co-funded by the EU through the European Maritime and Fisheries Fund (EMFF) within the National Program of collection, management, and use of data in the fisheries sector and support for scientific advice regarding the Common Fisheries Policy. We are grateful to two anonymous reviewers, for insightful comments that considerably improved the manuscript. We would like to thank our colleague Dr. Sophus zu Ermgassen for English style revision.

CONFLICT OF INTERESTS

All authors declare they have no conflict of interest.

AUTHOR CONTRIBUTIONS

JCB conceived the ideas and designed methodology; MLR collected the data; IAC analyzed the data; JCB wrote a first draft of the manuscript. All authors contributed critically to the drafts and gave final approval for publication.

ETHICAL STATEMENT

No specific authorization was required for any of the activities undertaken during this work. The study was conducted using statistical of the fishery and data available online.

DATA AVAILABILITY STATEMENT

The fisheries landing and environmental data that support the findings of this study are available from Supplementary Material Appendix S1.

ORCID

José Carlos Báez  <https://orcid.org/0000-0003-2049-0409>

Ivone A. Czerwinski  <https://orcid.org/0000-0001-8722-5285>

REFERENCES

- Báez, J. C., Fernández, F., Pascual, P., Ramos, M. L., & Abascal, F. (2018). *Updating the statistics of the EU-Spain purse seine fleet in the Indian Ocean (1990–2017)*. Submitted to 20th Working Party on Tropical Tunas (WPTT20), IOTC.IOTC-2017-WPTT20.
- Báez, J. C., Gimeno, L., Gómez-Gesteira, M., Ferri-Yáñez, F., & Real, R. (2013). Combined effects of the North Atlantic Oscillation and the arctic oscillation on sea surface temperature in the Alborán Sea. *PLoS One*, 8(4), e62201. <https://doi.org/10.1371/journal.pone.0062201>
- Báez, J. C., Ortiz De Urbina, J. M., Real, R., & Macías, D. (2011). Cumulative effect of the north Atlantic oscillation on age-class abundance of albacore (*Thunnus alalunga*). *Journal of Applied Ichthyology*, 27(6), 1356–1359. <https://doi.org/10.1111/j.1439-0426.2011.01799.x>
- Báez, J. C., Pascual-Alayón, P., Ramos, M. L., & Abascal, F. J. (2018). Tónidos tropicales: Calentamiento global y seguridad alimentaria, una visión global. *Revista De Biología Marina Y Oceanografía*, 53(1), 1–8. <https://doi.org/10.4067/S0718-19572018000100001>
- Banu, S., Guo, Y., Hu, W., Dale, P., Mackenzie, J. S., Mengersen, K., & Tong, S. (2015). Impacts of El Niño Southern Oscillation and Indian Ocean Dipole on dengue incidence in Bangladesh. *Scientific Report*, 5, 16105. <https://doi.org/10.1038/srep16105>
- Bastos, A., Janssens, I. A., Gouveia, C. M., Trigo, R. M., Ciais, P., Chevallier, F., ... Running, S. W. (2016). European land CO₂ sink influenced by NAO and East-Atlantic pattern coupling. *Nature Communications*, 7, 10315. <https://doi.org/10.1038/ncomms10315>
- Chavez, F. P., Ryan, J., Lluch-Cota, S. E., & Ñiquen, M. (2003). From anchovies to sardines and back, multidecadal change in the Pacific Ocean. *Science*, 299, 217–221. <https://doi.org/10.1126/science.1075880>
- Diankha, O., & Thiaw, M. (2016). Studying the ten years variability of *Octopus vulgaris* in Senegalese waters using generalized additive model (GAM). *International Journal of Fisheries and Aquatic Studies*, 4(3), 61–67.
- Edwards, A. W. F., & Cavalli-Sforza, L. L. (1965). A method for cluster analysis. *Biometrics*, 21(2), 362–375. <https://doi.org/10.2307/2528096>
- Erauskin-Extramiana, M., Arrizabalaga, H., Hobday, A. J., Cabré, A., Ibaibarriaga, L., Arregui, I., ... Chust, G. (2019). Large-scale distribution of tuna species in a warming ocean. *Global Change Biology*, 25(6), 2043–2060. <https://doi.org/10.1111/gcb.14630>
- Faillettaz, R., Beaugrand, G., Goberville, E., & Kirby, R. R. (2019). Atlantic Multidecadal Oscillations drive the basin-scale distribution of Atlantic bluefin tuna. *Science Advances*, 5, eaar6993. <https://doi.org/10.1126/sciadv.aar6993>
- FAO. (2016). *The state of world fisheries and aquaculture. Contributing to food security and nutrition for all*, 200 pp. Rome, Italy: FAO.
- Fonteneau, A. (1976). Note sur les problèmes d'identification du bigeye dans les statistiques de pêche. *Collective Volumen Scientific Papers ICCAT*, 1, 168–171.

- Hastie, T. J., & Tibshirani, R. J. (1990). *Generalized Additive Models*, Vol. 43, Boca Raton, Florida: . CRC Press.
- Hu, H., Wu, Q., & Wu, Z. (2018). Influences of two types of El Niño event on the Northwest Pacific and tropical Indian Ocean SST anomalies. *Journal of Oceanology and Limnology*, 36, 33–47. <https://doi.org/10.1007/s00343-018-6296-5>
- IATTC, Inter-American Tropical Tuna Commission (2015). *Fishery Status Report—Informe de la Situación de la Pesquería*. No. 13, La Jolla, CA, EEUU. 204 pp. Available from website: <https://www.iatcc.org/PDFFiles2/FisheryStatusReports/FisheryStatusReport13-2.pdf>. last access 05/05/2020.
- IATTC, Inter-American Tropical Tuna Commission (2016). *Tunas, billfishes and other pelagic species in the Eastern Pacific Ocean in 2015*. Fishery Status Report / Informe de la Situación de la Pesquería 14: 1–190. La Jolla, CA: Inter-American Tropical Tuna Commission / Comisión Interamericana del Atún Tropical. Available from website: https://www.iatcc.org/PDFFiles/FisheryStatusReports/_Spanish/FisheryStatusReport14.pdf. last access 05/05/2020.
- IOTC, Indian Ocean Tuna Commission (2016). *Resolution 16/01 on an interim plan for rebuilding the Indian Ocean yellowfin tuna stock*. Available from website: <https://iotc.org/cmm/resolution-1601-interim-plan-rebuilding-indian-ocean-yellowfin-tuna-stock>. last access 04/06/2020.
- Kanaji, Y., Tanabe, T., Watanabe, H., Oshima, T., & Okazaki, M. (2012). Variability in reproductive investment of skipjack tuna (*Katsuwonus pelamis*) in relation to the ocean-climate dynamics in the tropical eastern Indian Ocean. *Marine and Freshwater Research*, 63(8), 695–707. <https://doi.org/10.1071/MF11146>
- Kendall, M. G. (1955). *Rank correlation methods*. London, UK: Griffin.
- Killick, R., & Eckley, I. A. (2014). changepoint: An R package for changepoint analysis. *Journal of Statistical Software*, 58(3), 1–19. <http://www.jstatsoft.org/v58/i03/>
- Killick, R., Fearnhead, P., & Eckley, I. A. (2012). Optimal detection of changepoints with a linear computational cost. *Journal of the American Statistical Association*, 107(500), 1590–1598. <https://doi.org/10.1080/01621459.2012.737745>
- Killick, R., Haynes, K., & Eckley, I. A. (2016). *changepoint: An R package for changepoint analysis*. R Package Version, 2.2.2. <https://CRAN.R-project.org/package=changepoint>
- Kim, S. (2015). Effects of climate-induced variation in the catch distribution and biological characteristic of Skipjack tuna *Katsuwonus pelamis* in the Western and Central Ocean. *Korean Journal of Fisheries and Aquatic Sciences*, 48, 489–497.
- Kumar, P. S., Pillai, G. N., & Manjusha, U. (2014). El Niño Southern Oscillation (ENSO) impact on tuna fisheries in Indian Ocean. *SpringerPlus*, 3, 591. <https://doi.org/10.1186/2193-1801-3-591>
- Langley, A., Briand, K., Kirby, D., & Murtugudde, R. (2009). Influence of oceanographic variability on recruitment of yellowfin tuna (*Thunnus albacares*) in the western and central Pacific Ocean. *Canadian Journal of Fisheries and Aquatic Sciences*, 66, 1462–1477. <https://doi.org/10.1139/F09-096>
- Lehodey, P., Chai, F., & Hampton, J. (2003). Modelling climate-related variability of tuna populations from a coupled ocean–biogeochemical-populations dynamics model. *Fisheries Oceanography*, 12(4–5), 483–494. <https://doi.org/10.1046/j.1365-2419.2003.00244.x>
- Lezama-Ochoa, N., Murua, H., Hall, M., Román, M., Ruiz, J., Vogel, N., ... Sancristobal, I. (2017). Biodiversity and habitat characteristics of the bycatch assemblages in fish aggregating devices (FADs) and school sets in the eastern Pacific Ocean. *Frontiers in Marine Science*, 4, 265. <https://doi.org/10.3389/fmars.2017.00265>
- Lim, E.-P., & Hendon, H. H. (2017). Causes and predictability of the negative Indian Ocean dipole and its impact on the Niña during 2016. *Scientific Reports*, 7, 12619. <https://doi.org/10.1038/s41598-017-12674-z>
- Lima, M., & Naya, D. E. (2011). Large-scale climatic variability affects the dynamics skipjack tuna in the Western Pacific Ocean. *Ecography*, 34(4), 597–605.
- Mann, H. B. (1945). Nonparametric tests against trend. *Econometrica*, 13, 245–259. <https://doi.org/10.2307/1907187>
- Mantua, N. J., & Hare, S. R. (2002). The Pacific Decadal Oscillation. *Journal of Oceanography*, 58, 35–44.
- Mantua, N. J., Hare, S. R., Zhang, Y., Wallace, J. M., & Francis, R. C. (1997). A Pacific interdecadal climate oscillation with impacts on salmon production. *Bulletin of the American Meteorological Society*, 78, 1069–1079. [https://doi.org/10.1175/1520-0477\(1997\)078<1069:APICOW>2.0.CO;2](https://doi.org/10.1175/1520-0477(1997)078<1069:APICOW>2.0.CO;2)
- Marsac, F., & Demarcq, H. (2016). *Outline of climate and oceanographic conditions in the Indian Ocean, an update to mid-2016*. Submitted to 18th Working Party on Tropical Tunas (WPTT18), IOTC-2016-WPTT18-09.
- Mejuto, J. (2003). Recruit indices of the North Atlantic Swordfish (*Xiphias gladius*) and their possible link to atmospheric and oceanographic indicators during the 1982–2000 periods. *Collective Volume Scientific Papers ICCAT*, 55, 1506–1515.
- Ménard, F., Marsac, F., Bellier, E., & Cazelles, B. (2007). Climatic oscillations and tuna catch rates in the Indian Ocean, a wavelet approach to time series analysis. *Fisheries Oceanography*, 16(1), 95–104. <https://doi.org/10.1111/j.1365-2419.2006.00415.x>
- Newman, M., Alexander, M. A., Ault, T. R., Cobb, K. M., Deser, C., Di Lorenzo, E., ... Smith, C. A. (2016). The Pacific decadal oscillation, revisited. *Journal of Climate*, 29, 4399–4427. <https://doi.org/10.1175/JCLI-D-15-0508.1>
- Pallarés, P., García Mamolar, J. M., & Fernández, A. (1983). Composición por edades del rabal en las capturas de la flota tropical española. *Collective Volume Scientific Paper ICCAT*, 18(1), 106–110.
- Pianet, R., Pallarés, P., & Petit, C. (2000). *New sampling and data processing strategy for estimating the composition of catches by species and sizes in the European purse seine tropical tuna fisheries*. IOTC-WPDCS/2000/10.
- Robinson, J., Guillotreau, P., Jiménez-Toribio, R., Lantz, F., Nadzon, L., Dorizo, J., ... Marsac, F. (2009). *Impacts of climate variability on the tuna economy of Seychelles*. Available from Web Site, hal-00430051
- Rohit, P., Syda, R., & Rammohan, K. (2012). Age, growth and population structure of the yellowfin tuna *Thunnus albacares* (Bonnaterre, 1788) exploited along the east coast of India. *Indian Journal of Fisheries*, 59, 1–6.
- Rubio, C. J., Macías, D., Camiñas, J. A., Fernández, I. L., & Báez, J. C. (2016). Effects of the North Atlantic Oscillation on Spanish catches of albacore, *Thunnus alalunga*, and yellowfin tuna, *Thunnus albacares*, in the North-east Atlantic Ocean. *Animal Biodiversity and Conservation*, 39(2), 195–198. <https://doi.org/10.32800/abc.2016.39.0195>
- Torres-Faurieta, L., Dreyfus, M., & Rivas, D. (2016). Recruitment forecasting of yellowfin tuna in the eastern Pacific Ocean with artificial neuronal networks. *Ecological Informatics*, 36, 106–113. <https://doi.org/10.1016/j.ecoinf.2016.10.005>
- Vicente-Serrano, S. M., Trigo, R. M., López-Moreno, J. I., Liberato, M. L. R., Lorenzo-Lacruz, J., Beguería, S., ... El Kenawy, A. (2011). Extreme winter precipitation in the Iberian Peninsula in 2010, anomalies, driving mechanisms and future projections. *Climate Research*, 46, 51–65. <https://doi.org/10.3354/cr00977>
- Wang, S., Huang, J., He, Y., & Guan, Y. (2014). Combined effects of the Pacific Decadal Oscillation and El Niño–Southern Oscillation on Global Land Dry–Wet Changes. *Scientific Reports*, 4, 6651. <https://doi.org/10.1038/srep06651>
- Wheeler, M. C., & Hendon, H. H. (2004). An All-Season Real-Time Multivariate MJO Index: Development of an Index for Monitoring and Prediction. *Monthly Weather Review*, 132, 1917–1932. <https://doi.org/10.1175/1520-0493>

- Wieners, C. E., Dijkstra, H. A., & De Ruijter, W. P. M. (2017). The influence of the Indian Ocean on ENSO Stability and Flavor. *Journal of Climate*, 30, 2601–2620. <https://doi.org/10.1175/JCLI-D-16-0516.1>
- Wood, S. N. (2006). *Generalized additive models: An introduction with R*. Boca Raton, FL: CRC Press, Chapman and Hall.
- Wood, S. N. (2011). Fast stable restricted maximum likelihood and margin a likelihood estimation of semiparametric generalized linear models. *Journal of the Royal Statistical Society (B)*, 73, 3–36. <https://doi.org/10.1111/j.1467-9868.2010.00749.x>
- Yan, H., Sun, L., Wang, Y., Huang, W., Qiu, S., & Yang, C. (2011). A record of the Southern Oscillation Index for the past 2,000 years from precipitation proxies. *Nature Geoscience*, 4(9), 611–614. <https://doi.org/10.1038/NCEO1231>
- Yang, G., Liu, L., Zhao, X., Li, Y., Duan, Y., Liu, B., ... Yu, W. (2019). Impacts of different types of ENSO events on thermocline variability in the Southern Tropical Indian Ocean. *Geophysical Research Letters*, 46(12), 6775–6785. <https://doi.org/10.1029/2019GL082818>
- Zhang, C. (2005). Madden-Julian oscillation. *Reviews of Geophysics*, 43, RG2003. <https://doi.org/10.1029/2004RG000158>
- Zhou, X., Alves, O., Marsland, S. J., Bi, D., & Hirst, A. C. (2017). Multi-decadal variations of the South Indian Ocean subsurface temperature influenced by Pacific Decadal Oscillation. *Tellus A, Dynamic Meteorology and Oceanography*, 69, 1. <https://doi.org/10.1080/16000870.2017.1308055>
- Zuur, A. F., Ieno, E. N., & Elphick, C. S. (2010). A protocol for data exploration to avoid common statistical problems. *Methods in Ecology and Evolution*, 1, 3–13. <https://doi.org/10.1111/j.2041-210X.2009.00001.x>
- Zuur, A. F., Ieno, E. N., Walker, N. J., Saveliev, A. A., & Smith, G. M. (2009). *Mixed effects models and extensions in ecology with R. Statistics for biology and health*. New York, NY: Springer. <https://doi.org/10.1007/978-0-387-87458-6>
- Zwolinski, J. P., Emmett, R. L., & Demer, D. A. (2011). Predicting habitat to optimize sampling of Pacific sardine (*Sardinops sagax*). *ICES Journal of Marine Science*, 68(5), 867–879. <https://doi.org/10.1093/icesjms/fsr038>

SUPPORTING INFORMATION

Additional supporting information may be found online in the Supporting Information section.

How to cite this article: Báez JC, Czerwinski IA, Ramos ML. Climatic oscillations effect on the yellowfin tuna (*Thunnus albacares*) Spanish captures in the Indian Ocean. *Fish Oceanogr*. 2020;00:1–12. <https://doi.org/10.1111/fog.12496>